Remote estimation of nitrogen fixation by *Trichodesmium*

Raleigh R. Hood[a,*], Ajit Subramaniam[b,1], Linda R. May[a], Edward J. Carpenter[c], Douglas G. Capone[b]

[a] *Center for Environmental Science, University of Maryland, Horn Point Laboratory, Cambridge, MD 21613-0775, USA*
[b] *Wrigley Institute for Environmental Studies, USC, Los Angeles, CA 90089, USA*
[c] *Romberg Tiburon Center, San Francisco State University, Tiburon, CA 94920, USA*

Accepted 16 June 2001

Abstract

A non-spectral model is described that can be used to calculate N_2-fixation rate from remote estimates of *Trichodesmium* biomass. This model, which is similar to formulations that have been developed for estimating primary production from satellite-derived phytoplankton chlorophyll concentrations, is parameterized using measured *Trichodesmium* N_2-fixation vs. irradiance (I) data and observed subsurface *Trichodesmium* biomass profiles from the Tropical Atlantic Ocean. These data reveal that the N_2-fixation vs. I responses and subsurface distributions of *Trichodesmium* vary substantially in tropical waters. The calculated rates are sensitive to only one of three forcing variables: the remotely sensed *Trichodesmium* chlorophyll concentration, B_T^{sat}, and two of the model parameters: the maximum N_2-fixation rate, $P_{max}^{B_T}$, and the depth of the subsurface *Trichodesmium* biomass maximum, Z_m. The model is particularly sensitive to the latter. These results suggest that in order to generate N_2-fixation rate estimates with reasonable confidence limits with this model, means must be sought to account for in situ variablity in $P_{max}^{B_T}$ and Z_m. A series of correlation analyses reveal statistically significant correlations between the diffuse attenuation coefficient, K_{par}, and $P_{max}^{B_T}$, and between wind speed and Z_m. These relationships are suggested as potential means of accounting for natural variability in $P_{max}^{B_T}$ and Z_m. An example remote sensing-based rate calculation is made using SeaWiFS-derived *Trichodesmium* chlorophyll concentration in the South Atlantic Bight described in Subramaniam et al., 2002 (Deep-Sea Research, 2002). Although the optical conditions in the Bight were not all within the range used to derive the model parameters, the model gives rates that are consistent with direct rate measurements in *Trichodesmium* blooms. Because *Trichodesmium* biomass can only be detected remotely at relatively high concentrations, efforts to estimate global rates with this model will require the use of both shipboard and satellite data. © 2001 Published by Elsevier Science Ltd.

*Corresponding author. Tel.: +1-410-228-8200; fax: +1-410-221-8490.

E-mail address: raleigh@hpl.umces.edu (R.R. Hood).

[1] Now at ESSIC, University of Maryland, College Park, MD 20742, USA.

1. Introduction

Eppley and Petersen (1979) stated that external sources of nitrogen (N), such as N_2-fixation and atmospheric N deposition, were required to effect a net transport of atmospheric CO_2 from the upper ocean to the deep sea because NO_3 from depth is transported upwards with dissolved inorganic carbon (DIC) in approximate Redfield proportions. While some early estimates (Capone and Carpenter, 1982) suggested a relatively small role for N_2-fixation in the ocean, more recent observations and analyses indicate that N_2-fixation is, in fact, a globally significant source of new N (Carpenter and Romans, 1991; Galloway et al., 1995; Michaels et al., 1996; Karl et al., 1997; Gruber and Sarmiento, 1997; Capone et al., 1997). Indeed, it has been suggested (Hood et al., 2000) that N_2-fixation is responsible for virtually all of the biologically mediated net annual carbon export to the deep ocean (i.e. that amount exported less DIC transported up from depth). In addition, the global balance between N_2-fixation and denitrification ultimately controls the size of the oceanic N pool and therefore impacts the degree to which the oceans are either nitrogen or phosphorus limited (Codispoti, 1989; Falkowski, 1997; Tyrrell, 1999). Thus marine nitrogen fixation is potentially important in the global carbon cycle, and it is a key process which directly impacts nutrient limitation and ocean productivity. Yet there is considerable uncertainty in current global N_2-fixation rate estimates, which vary from 10 to 200 Tg N yr^{-1} (Gruber and Sarmiento, 1997; see their Table 3).

The conspicuous marine cyanobacterium, *Trichodesmium*, has long been recognized as an important N_2-fixer in the open ocean. Direct regional and global estimates of oceanic N_2-fixation rate have been based largely on ^{15}N uptake and acetylene reduction rate measurements on individual *Trichodesmium* colonies, which are then scaled up to volume and area using microscope-derived colony concentration estimates from shipboard plankton surveys (e.g. Capone and Carpenter, 1982; Capone et al., 1997; Carpenter et al., 2002). The extent of these surveys is extremely limited (see Capone et al., 1997, their Fig. 2), and they do not provide sufficient coverage of the oceans to characterize adequately the considerable temporal and spatial variability of *Trichodesmium* populations. Because of obvious limits on shiptime and human resources, it is unlikely that this problem can be rectified in the foreseeable future. Therefore, alternative means must be sought that can provide the temporal and spatial coverage required to decrease the uncertainty in regional and global rate estimates.

One possible solution is to use remote sensing to extend the spatial and temporal coverage of the shipboard measurements. As described by Subramaniam et al. (2002), it is now feasible to detect and estimate the biomass of *Trichodesmium* populations using upwelling radiance measurements from ocean color sensors such as Sea-viewing wide Field-of-view Sensor (SeaWiFS). This is made possible by two unique optical characteristics of this organism: absorption and fluorescence by the accessory pigment phycoerythrin (which can be detected in the non-linearity of the slope of the remote sensing reflectance spectrum at the 490, 510 and 555 nm SeaWiFS wavebands), and strong backscattering by gas vacuoles that are present in the individual cells (which can be assessed using the absolute magnitude of the remote sensing reflectance at these same SeaWiFS bands). Although this organism is not the only diazotrophic species in the ocean, it is likely one of the most significant contributors to global ocean N_2-fixation (Capone et al., 1997). The idea, then, is to use remotely sensed *Trichodesmium* biomass estimates as the basis for estimating N_2-fixation rates over large spatial and temporal scales in much the same way that global phytoplankton production rates are estimated

from remote estimates of phytoplankton chlorophyll concentration (e.g. Sathyendranath et al., 1995; Longhurst et al., 1995; Behrenfeld and Falkowski, 1997).

It is well known that there are large uncertainties in rate estimates derived from satellite measurements of chlorophyll concentration (Banse and Yong, 1990). The two major difficulties are (1) inaccuracies in satellite-based estimates of the biomass (chlorophyll concentration) and (2) in situ variability in the physiological "constants" utilized in the models. However, the application of this approach to *Trichodesmium* potentially has two distinct advantages. First, because *Trichodesmium* biomass is generally restricted to the upper 50 m of the water column, and because this organism is only found in relatively clear ($K_{par} < 0.13$ m^{-1}) coastal and open-ocean waters (Capone et al., 1997), satellite color sensors should be able to "see" a large fraction of the biomass in the water column. Thus, there will be few cases where a large fraction of the population is not detected by the sensor, as is often the case with phytoplankton. Second, because the goal is to model the production of a monospecific population, the complication of physiological variability associated with different species compositions of different ocean regions is avoided; i.e. one only needs to account for parameter variability due to intraspecific physiological variability. Thus, there is reason to believe that it might be possible to estimate rates of *Trichodesmium* N$_2$-fixation more accurately from space than total primary production.

In this paper a simple model is described that can be used to estimate N$_2$-fixation rates from remote *Trichodesmium* biomass estimates. Sensitivity analyses show that this model, which is based upon measured N$_2$-fixation vs. I response curves and subsurface distribution profiles of natural marine *Trichodesmium* populations in Tropical Atlantic waters, is relatively insensitive to variability in all but a few key parameters. In particular, proper specification of the maximum rate of N$_2$-fixation and the depth of the population maximum are crucial to generate accurate rate estimates. It is also shown that the model is insensitive to two forcing variables, the surface irradiance and the diffuse attenuation coefficient, which are commonly included in productivity models. A test rate calculation is made on the *Trichodesmium* bloom in the South Atlantic Bight (SAB) described by Subramaniam et al. (2002), which suggests rates of 14–113 μmol N m^{-2} h^{-1}. Although the optical conditions in the SAB were not all within the range used to derive the model parameters, these rates are consistent with the limited number of direct rate measurements that have been made in *Trichodesmium* blooms.

2. Modeling approach

The basic modeling approach followed here is a non-linear, non-spectral, "semi-analytical" method similar to that described in Platt et al. (1988). The vertically integrated N$_2$-fixation rate, N_{fix}^{int}, is estimated as follows:

$$N_{fix}^{int} = \int B_T(Z) \times P^{B_T}(Z)\,dZ. \tag{1}$$

The vertical distribution of *Trichodesmium* biomass, $B_T(Z)$, is described by a simple Gaussian function

$$B_T(Z) = \frac{h}{\sigma(2\pi)^{1/2}} \exp\left(-\frac{(Z - Z_m)^2}{2\sigma^2}\right), \tag{2}$$

where Z_m is the depth of the subsurface biomass maximum, σ defines the breadth of the vertical distribution, and h is the total biomass (area) under the curve. This function differs from that used by Platt et al. (1988) (and in subsequent publications) in that it lacks the "background biomass" parameter, B_0. B_0 was omitted in this application because it was not required to fit the observed *Trichodesmium* biomass profiles, which tend to decrease to zero above and below the subsurface biomass maximum (see Fig. 4 below).

The biomass normalized N_2-fixation rate is described as a function of depth $P^{B_T}(Z)$ using a three-parameter, non-linear, N_2-fixation vs. I function, which includes photoinhibition (Platt et al., 1980)

$$P^{B_T}(Z) = P_s^{B_T}(1 - e^{-I(Z)/I_s})e^{-I(Z)/I_b}. \tag{3}$$

In (3) $P_s^{B_T}$ is a parameter which is related to the parameter $P_{max}^{B_T}$, the maximum N_2-fixation rate normalized to *Trichodesmium* chlorophyll

$$P_{max}^{B_T} \equiv P_s^{B_T}\left(\frac{\alpha^{B_T}}{\alpha^{B_T} + \beta^{B_T}}\right)\left(\frac{\beta^{B_T}}{\alpha^{B_T} + \beta^{B_T}}\right)^{I_s/I_b}, \tag{4}$$

where α^{B_T} defines the increase in N_2-fixation rate with increasing irradiance at low light intensities and β^{B_T} is the photoinhibition parameter (Platt et al., 1980). $I_s = P_s^{B_T}/\alpha^{B_T}$ is an analogous parameter to the conventional index of light adaptation, I_k, and $I_b = P_s^{B_T}/\beta^{B_T}$ is an index of photoinhibition (Platt et al., 1980; see their Fig. 7). Because $P_s^{B_T}$ is, in part, a function of β^{B_T} and vice versa these two parameters are much more variable when fitted to measured curves than their counterparts $P_{max}^{B_T}$ and I_b. The shape of the N_2-fixation vs. I relationship is therefore specified in the model using $P_{max}^{B_T}$, I_b and α^{B_T}, and then fixed point iteration (Goffman, 1962) is used to solve for β^{B_T}, which can then be used to calculate $P_s^{B_T} = I_b \times \beta^{B_T}$ and I_s for (3). Finally, in (3)

$$I(Z) = I_0 e^{-K_{par}Z}, \tag{5}$$

where K_{par} is the diffuse attenuation coefficient for photosynthetically active radiation (PAR) and I_0 is PAR at the sea surface. Thus, if I_0 and K_{par} are known (i.e. considered as forcing variables) then $P^{B_T}(Z)$ in (1) can be determined if the N_2-fixation vs. I parameters $P_{max}^{B_T}$, I_b and α^{B_T} can be specified.

The *Trichodesmium* chlorophyll concentration measured by the satellite, B_T^{sat}, can be approximately related to the subsurface biomass profile as

$$B_T^{sat} = \frac{\int_0^{Z_{90}} B_T(Z)e^{-2K_{par}Z}\,dZ}{\int_0^{Z_{90}} e^{-2K_{par}Z}\,dZ}, \tag{6}$$

where the penetration depth, $Z_{90} = 1/K_{par}$, is the optical depth at which the downwelling irradiance falls to $1/e$ (Gordon and Clark, 1980; cf. Banse and Yong, 1990). The relation is approximate because it is derived by assuming a vertically uniform K_{par}. Then substituting (2) into (6) and solving for h gives

$$h = \frac{\sigma(2\pi)^{1/2} B_T^{sat} \int_0^{Z_{90}} e^{-2K_{par}Z}\,dz}{\int_0^{Z_{90}} \exp\left(-(Z - Z_m)^2/2\sigma^2\right)e^{-2K_{par}Z}\,dz}. \tag{7}$$

Thus if the two shape parameters, σ and Z_m, in (2) can be specified, then (7) can be used to numerically calculate h from B_T^{sat} (cf. Platt and Sathyendranath, 1988), which determines $B_T(Z)$.

Table 1
Forcing variables and model parameters, symbols and units

Description	Symbol	Units
Forcing variables		
Surface irradiance (PAR)	I_0	$\mu E\ m^{-2}\ s^{-1}$
Diffuse attenuation coefficient (PAR)	K_{par}	m^{-1}
Satellite-derived *Trichodesmium* chlorophyll	B_T^{sat}	$mg\ m^{-3}$
Model parameters		
Normalized maximum N_2-fixation rate	$P_{max}^{B_T}$	$\mu mol\ N(mg\ chl\ h)^{-1}$
Light-limited slope	α^{B_T}	$\mu mol\ N(mg\ chl\ h)^{-1}(\mu E\ m^{-2}\ s^{-2})^{-1}$
Photoinhibition parameter	I_b	$\mu E\ m^{-2}\ s^{-1}$
Width of the subsurface distribution	σ	m
Depth of the biomass maximum	Z_m	m

The vertically integrated rate can then be calculated by numerically integrating (1) using the satellite-derived $B_T(Z)$, with $P^{B_T}(Z)$ specified as described above.

This model is essentially the same as that described in Platt et al. (1988) except that it lacks the background biomass parameter, B_0, it is integrated numerically rather than analytically, and it is parameterized specifically for *Trichodesmium* (see Section 3). The forcing variables required to run the basic model include the surface PAR, I_0, the diffuse attenuation coefficient for PAR, K_{par}, and an estimate of the near-surface *Trichodesmium* chlorophyll concentration, B_T^{sat} (Table 1). All of these can be derived remotely, i.e. I_0 can be estimated using radiative transfer models (e.g. Sathyendranath and Platt, 1988), B_T^{sat} can be estimated from SeaWiFS (Subramaniam et al., 2002), and K_{par} can be empirically related to SeaWiFS-derived K_{490} (see Eq. (10) below). The model parameters are $P_{max}^{B_T}$, I_b and α^{B_T}, which specify the N_2-fixation rate vs. I relationship, and σ and Z_m, which specify the subsurface biomass profile.

For the rate calculations in this paper the model was integrated over 200 m depth using Euler's method with $\Delta Z = 0.25$ m

3. Model parameterization and sensitivity

In this section a data base that was collected in the tropical western Atlantic from 23 May–18 June 1994 (Fig. 1) is used to develop an initial set of model parameters and assess the impact of natural variability in these parameters and the forcing variables on the modeled N_2-fixation rates. These data are ideal for this purpose because they include all of the basic measurements required to parameterize and force the model. In addition, they were collected over a relatively wide range of conditions; from open-ocean tropical Atlantic waters to more shallow coastal/island regions in the Bahamas and the Antilles Archipelago (Fig. 1). The focus here is on three aspects of the data: N_2-fixation rate vs. I curves measured using the acetylene reduction technique, the subsurface *Trichodesmium* chlorophyll profiles estimated from microscope counts of colony concentrations, and the forcing variables, I_0 and K_{par}. Here we provide a brief overview of the methods used to
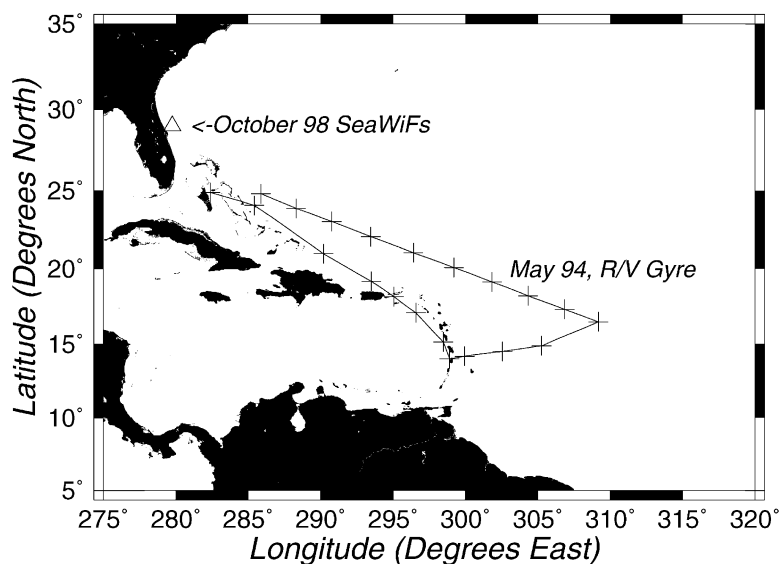
Fig. 1. Map of the northwestern, tropical and subtropical Atlantic, showing the cruise track of the May 1994, R.V. Gyre cruise. The data collect on this cruise were used to develop the initial formulation and parameterization of the N_2-fixation rate estimation model. Also shown is the location of the *Trichodesmium* bloom that was observed remotely in the South Atlantic Bight by Subramaniam et al. (2002) and used for a test application of the model.

generate these data. The reader is referred to Capone (1993) and Carpenter et al. (2002) for a more detailed description of the methods.

Water samples for *Trichodesmium* abundance measurements were collected using a CTD Rosette system with 10-l Niskin bottles. Samples were typically collected at 5 depths corresponding to 100%, 55%, 28%, 10%, 1.3% I_0 using extinction coefficients measured the previous day. Colony concentrations at each station were determined by gravity filtering 10 l of seawater from the Rosette casts onto an 8- or 10-μm pore size, 47-mm diameter, nuclepore or poretics filter. Direct filtration by gravity allowed minimal disturbance to colonies. The filter was mounted on an oversize (75 mm × 50 mm × 1 mm) glass microscope slide and *Trichodesmium* colonies were then enumerated on ship within 24 h of collection. Counts were done at 400 × magnification using a Zeiss Axioskop microscope with epifluorescence and green excitation. *Trichodesmium* chlorophyll concentration was estimated from colony concentrations using a conversion factor of 50 ng chl/colony for large colonies and 20 ng chl/colony for small colonies (Carpenter et al., 2002.). The 20 ng chl/colony conversion was used at only six stations sampled on 1–6 June in low salinity waters where a distinct population of smaller colonies was observed.

Eq. (2) was fitted to the resulting 18 subsurface *Trichodesmium* chlorophyll profiles using a non-linear, least-squares method, except in 4 cases where two distinct subsurface maxima were observed. These latter profiles were omitted from the analysis (all of the fitted profiles are plotted together in Fig. 4). A B_T^{sat} value was estimated for each of the fitted *Trichodesmium* chlorophyll profiles using (6), and these were used to characterize the variability in this forcing parameter (Table 2). All of the K_{par} data used in the analyses described below were determined at noon using

Table 2
Statistics on cruise-derived model parameters and forcing variables

Parameter	Mean	Median	Range	Std/Mean	n
N₂-fixation vs. I parameters					
$P^{B_T}_{max}$	3.19	2.57	0.64–10.0	0.78	17
α^{B_T}	0.023	0.017	0.003–0.092	1.0	17
I_b	1195	813.1	266.2–3519	0.92	10
Trichodesmium profile shape parameters					
σ	11.13	7.58	4.10–25.9	0.65	14
Z_m	12.29	12.00	0–38	0.99	14
Forcing variables					
I_0	1022	1036	792–1174	0.09	26
K_{par}	0.040	0.037	0.028–0.071	0.28	24
B^{sat}_T	0.628	0.119	0–2.705	1.44	14

a Biospherical Instruments Spectroradiometer (MER1000). The variability in these data is characterized in Table 2 as well. In addition, the wind speed measurements used in the correlation analyses described in Section 4.2 below were extracted from the shipboard sail system that continuously records, among other things, wind speed data from the ship's anemometer.

Trichodesmium N₂-fixation rates were determined using the acetylene reduction technique (Capone, 1993) on isolated colonies collected at 10–20 m by slow (1 knot) plankton tows using a 1-m diameter, 202-µm mesh net. Colonies were incubated from 10:00 AM to 2:00 PM local time at 100%, 55%, 28%, 10%, 1.3% I_0 in surface water cooled deck incubators. The subsurface irradiance levels were approximated using neutral density filters. Acetylene reduction rates were converted to mol N fixed using a 3 : 1 ratio of C_2H_2 reduced to N_2 fixed. Usually only one N₂-fixation vs. *I* incubation was performed at each station location (Fig. 1). The absolute irradiance (µE m⁻² s⁻¹) for generating N₂-fixation vs. *I* curves was determined by averaging the ship-measured surface PAR over the approximate incubation period of N₂-fixation rate incubations. These average noon-time I_0 values also were used to quantify the variability in the surface irradiance conditions during the cruise (Table 2). The average values were then multiplied by the attenuation coefficients for each simulated in situ light depth to derive the irradiance for the N₂-fixation vs. *I* curves.

The rates were also normalized to *Trichodesmium* chlorophyll concentration using the conversions described above, i.e. the measured rates were divided by the total chlorophyll concentration estimated from the number of colonies incubated at each light level. Because several of the curves had a significant positive values at 1.3% I_0 after normalization, the chlorophyll-normalized rates measured at 1.3% I_0 for each curve were subtracted from the normalized rates at all light levels. i.e. the positive intercept was subtracted off. Eq. (3) was then fitted to the data from each of the 17 experiments again using a non-linear least-squares method. However, in 7 cases no photoinhibition was observed. In these circumstances the photoinhibition parameter, β^{B_T}, was specified to be zero. All of the fitted curves are plotted together in Fig. 2. It can be seen that these fitted curves provide rather crude characterizations of the N₂-fixation vs. *I* responses, with only five points per curve, and in some cases less. Moreover, these curves provide no information about
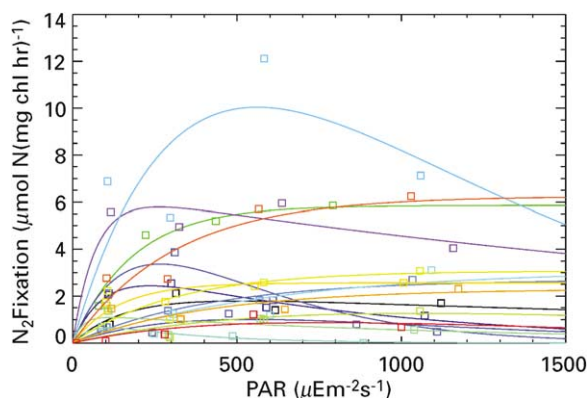
Fig. 2. N_2-fixation vs. I curves fitted to the data collected on the R.V. Gyre cruise. There are a total of 17 curves. Each curve was fitted with Eq. (3), either with or without photoinhibition depending upon whether or not photoinhibition was observed (see Section 3 in text for details). The colors of the curves correspond to the colors of the actual measured points to which they were fitted.

vertical variability in the N_2-fixation vs. I response of *Trichodesmium*. They may, in fact, be biased because populations from the subsurface maximum were incubated over a range of light intensities that they might not normally experience. Efforts are currently being undertaken to collect short-term "photosynthetron" N_2-fixation vs. I measurements at multiple depths, which will provide much more highly resolved light response data on *Trichodesmium* for use in future modeling and rate estimation efforts. But until these data are available, these measurements have to suffice.

It should be noted that the contribution of free filaments ("trichomes") was not taken into account in either the *Trichodesmium* chlorophyll estimates or the N_2-fixation rate measurements that were used in the following analyses. This is justified because the results from assessments of the proportion of free filaments compared to colonies from three cruises to these waters (the R.V. Gyre cruise included, plus two more recent expeditions) has shown that free filaments constitute a relatively small fraction of the total *Trichodesmium* biomass for stations with appreciable *Trichodesmium* densities. Across all stations and all depths (inclusive—115 discrete observations), trichomes in colonies averaged 1432 trichomes/l while free trichome densities were on average 144 trichomes/l, or 9% of total filaments. However, it should be recognized that N_2-fixation vs. I curves and the subsurface *Trichodesmium* biomass profiles described in this study are biased toward colonies and may not, therefore, be representative of populations that are composed of a large fraction of free trichomes.

In the following sections the sensitivity of the model to natural variations in the forcing variables (I_0, K_{par}, B_T^{sat}) and the model parameters ($P_{max}^{B_T}$, α^{B_T}, I_b, σ and Z_m) was determined by simultaneously varying two, related parameters (e.g. $P_{max}^{B_T}$ vs. α^{B_T}) over the observed range of variability while holding the rest of the parameters at their mean values (as specified in Table 2).

3.1. N_2-fixation rate vs. I variability and model sensitivity

Of the three N_2-fixation vs. I parameters, α^{B_T} is the most variable, $P_{max}^{B_T}$ is the least and I_b is intermediate, and all of them vary by more than a factor of 10 (Table 2). It should be noted,

however, that the statistics for I_b are biased because this parameter is not defined in 7 of the 17 experiments where no photoinhibition was observed. Thus, the variability in I_b is probably greater than reported in Table 2.

Fig. 3A shows that the model is relatively insensitive to natural variations in I_b and generally more sensitive to variations in $P_{max}^{B_T}$. (The grey-shaded area, where the maximum rate of N_2-fixation is high and there is strong photoinhibition, represents the parameter space where the fixed-point iteration does not converge to a solution. Thus, the model cannot be used to estimate N_2-fixation rates for photoresponses in this parameter space. A similar, though
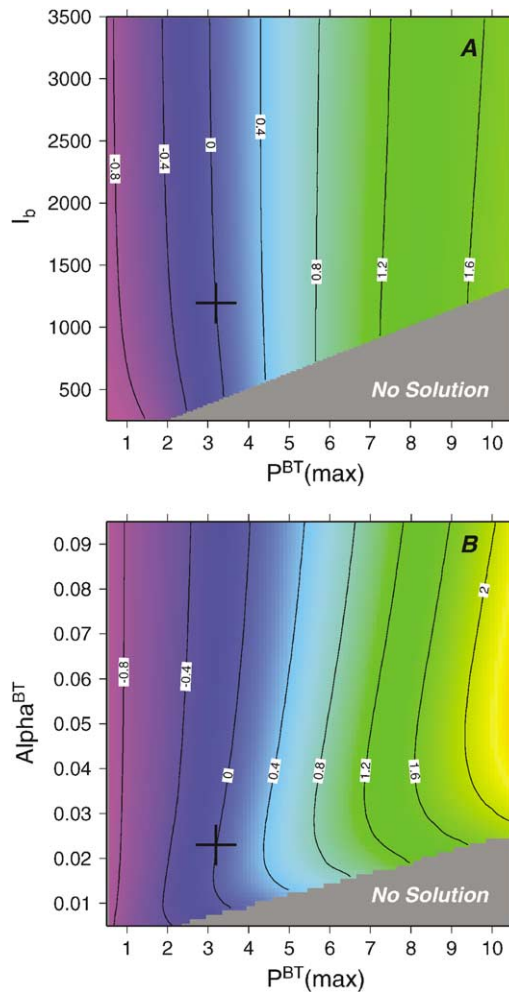

Fig. 3. The deviation (or "error") of the model-calculated rate from the mean rate when (A) $P_{max}^{B_T}$ and I_b, and (B) $P_{max}^{B_T}$ and α^{B_T} are varied over the ranges observed during the R.V. Gyre cruise (Table 2). The deviation is defined as $(R - R_m)/R$, where R is the rate determined for various combinations of $P_{max}^{B_T}$ and I_b, with all other model parameters held constant at their cruise mean values (Table 2). The mean rate, R_m, (denoted by a +) was calculated using all of the mean parameter values and forcing variables from Table 2.

somewhat smaller, "null" parameter space is apparent in Fig. 3B where $P_{max}^{B_T}$ is large and α^{B_T} small). The model is also relatively insensitive to in situ changes in α^{B_T} (Fig. 3B), but with α^{B_T} there is a significant interaction with $P_{max}^{B_T}$. i.e. the model is more sensitive to α^{B_T} when α^{B_T} is low and $P_{max}^{B_T}$ is high.

This pattern of sensitivity (most sensitive to $P_{max}^{B_T}$, less sensitive to α^{B_T}, and insensitive to I_b) is consistent with circumstances where the bulk of the population is centered at a depth where light levels are at or somewhat above I_k (which is, in fact, the case, see Section 3.3 below). Under these conditions the population is shallow enough so that it is not strongly light-limited (leading to low sensitivity to α^{B_T}), but deep enough to avoid significant photoinhibition (leading to insensitivity to I_b). One would expect to see increasing sensitivity to I_b and decreasing sensitivity to α^{B_T} with decreasing Z_m and increasing I_0. In contrast, one would expect to see increasing sensitivity to α^{B_T} and decreasing sensitivity to $P_{max}^{B_T}$ with increasing Z_m and decreasing I_0. The increase in the sensitivity to α^{B_T} with increasing $P_{max}^{B_T}$ at low α^{B_T} happens because increasing $P_{max}^{B_T}$ effectively increases I_k; i.e. it moves the rate calculation from light saturation to light limitation.

It should be emphasized that with the forcing variables and model parameters set at their mean values, the model is quite sensitive to variations in $P_{max}^{B_T}$. For example, if the mean $P_{max}^{B_T}$ from Table 2 were used in the model to calculate rates at all of the R.V. Gyre stations (Fig. 1), it could result in errors that are greater than 150% (Fig. 3). Errors of this type will be particularly acute when a $P_{max}^{B_T}$ value is assumed that is greater than the true in situ value (Fig. 3). One potential means of accounting for some fraction of the observed variability in $P_{max}^{B_T}$ is discussed in Section 4.1 below.

The sensitivity of general productivity models to variations in the P vs. I parameters has been studied extensively in a series of publications by T. Platt, S. Sathyendranath and co-workers (e.g. Platt et al., 1988, 1990, 1991; Sathyendranath et al., 1989). Platt et al. (1988) showed that their model, which is based upon a similar set of equations, has a similar response to deviations in P_{max}^{B} from the mean, but in their case the maximum error was less than 50% for P_{max}^{B} varying by a factor of about 30 (see their Fig. 8A), whereas in this case the maximum error exceeds 150% for $P_{max}^{B_T}$ varying by about a factor of 16 (Fig. 3). It is possible that this difference in the sensitivities of the models is simply due to the fact that a different suite of mean parameter values (for *Trichodesmium* instead of phytoplankton) was used in this analysis. Thus, these differences in sensitivity may reflect real physiological and distributional differences between *Trichodesmium* and other phytoplankton species which has a negative impact on model performance.

Platt et al. (1988) also showed that the sensitivity of their model to variations in α^{B_T} is strongly dependent upon light flux, and that such models are not sensitive to α^{B_T} when irradiance is high, as suggested above. The relative insensitivity of the model to I_b shown here is consistent with the results of Platt et al. (1990), who showed analytically (assuming a vertically uniform biomass profile) that errors associated with variations in the photoinhibition parameter, β, should not generally exceed 10%, for phytoplankton. For *Trichodesmium*, which are less easily photo-inhibited than most phytoplankton species, the errors associated with variations in I_b should be even less. Subramaniam et al. (1999a) showed that *Trichodesmium* can dump excess energy readily as fluorescence and maintains relatively high internal concentrations of photoprotective pigments. In fact, the photoinhibition seen in some of the curves shown in Fig. 2 may be an artifact of trapping colonies at high light in incubators on the deck of the ship.

3.2. Subsurface profile variability and model sensitivity

The shape of the subsurface *Trichodesmium* chlorophyll distribution is also quite variable (Fig. 4 and Table 2). The width parameter, σ, varies between about 4 and 26 m, and the depth of the biomass maximum, Z_m, varies between 0 and 38 m. (note that the actual width of the subsurface distribution at the axis is approximately 4σ, Platt et al., 1988) Of the two, Z_m shows the most relative variability (Table 2).

The model-calculated rates are very sensitive to Z_m and less sensitive to σ, and there is a small, but significant interaction between them (Fig. 5), i.e. the model tends to be more sensitive to σ at extreme Z_m values, and more sensitive to Z_m when σ is small. Errors in estimated rates will be particularly large in cases where a Z_m value is assumed to be significantly greater than the true in situ Z_m (Fig. 5); the errors increase exponentially. For example, given the cruise mean parameter values, overestimation of Z_m by 10 m results in overestimation of the integrated rate by about a factor of two.

The model is particularly sensitive to Z_m because the estimation of h using (7) is critically dependent upon the value of Z_m (note that Z_m appears in the exponent of a vertical integral in the denominator of (7)). That is, the determination of h requires proper representation of the intersection between the Gaussian biomass distribution and the depth to which the satellite can
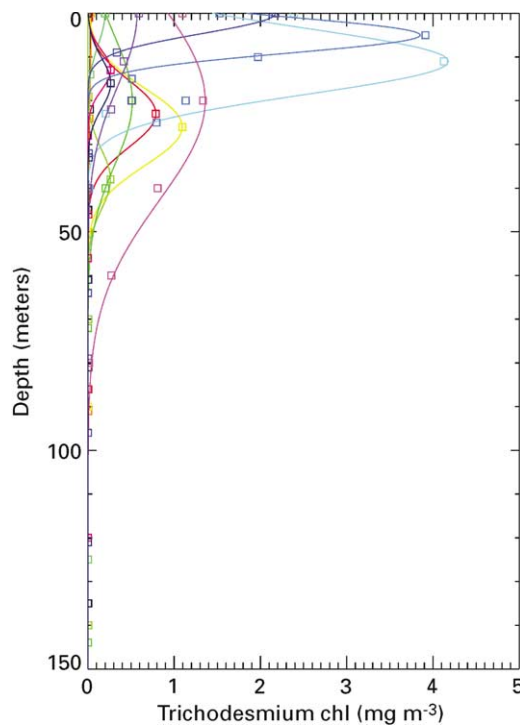

Fig. 4. Subsurface *Trichodesmium* biomass profiles expressed as *Trichodesmium* chlorophyll concentration measured on the R.V. Gyre cruise. Each of the 14 profiles, was fitted with Eq. (2). The colors of the curves correspond to the colors of the actual measured points to which they were fitted. (Two of the profiles collected on the cruise were not fitted with (2) and are not shown because they contained two subsurface maxima).
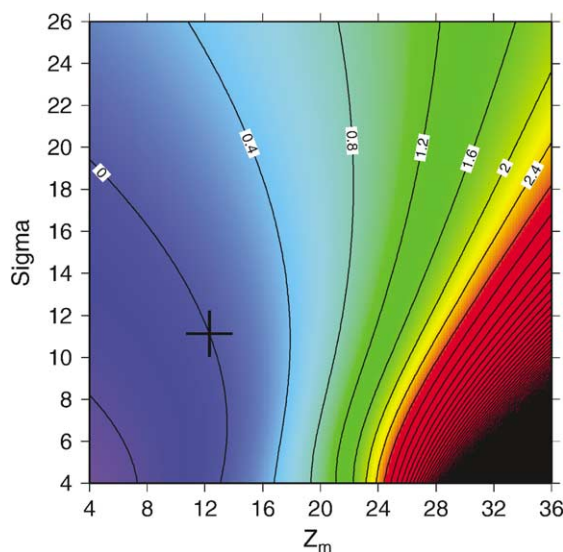
Fig. 5. As in Fig. 3 for Z_m vs. σ with ranges taken from Table 2.

see. When the assumed Z_m is greater than the true value, the model "thinks" that B_T^{sat} represents a smaller fraction of the subsurface maximum than it actually does and, as a result, calculates much more mass in the maximum than there actually is. Although the reverse happens when the assumed Z_m is smaller than the true value, the error does not increase exponentially (Fig. 5). The asymmetry in the sensitivity to Z_m depicted in Fig. 5 also arises because, when the biomass maximum is nearer to the surface, the N_2-fixation vs. I response is more saturated, and therefore errors in the depth of the maximum and errors in the estimation of h do not impact the calculated rates nearly as much. Thus, a general strategy for minimizing errors associated with the specification of the subsurface profile is to try to avoid overestimating Z_m. One potential means of accounting for some of the observed variability in Z_m, is discussed further in Section 4.2.

For comparison, Platt et al. (1988) similarly showed a relatively modest sensitivity to σ and a much stronger sensitivity to Z_m. However, their model appears to be less sensitive to both of these parameters, and in the case of Z_m the errors in their model actually decline at the deepest Z_m values (see their Fig. 7C) whereas they continue to increase exponentially in Fig. 5. These differences in the sensitivities of the two models to the biomass profile parameters may be due to the absence of a background biomass, B_0, in (2). As discussed above, this parameter was omitted in this application because it was not required to fit the observed *Trichodesmium* biomass profiles. Thus, although the absence of B_0 confers the advantage of reducing the number of parameters in the model by one, its removal from the equations appears to substantially increase the sensitivity of the model to the other profile parameters.

3.3. Forcing variability and model sensitivity

Table 2 shows that the variability in I_0 and K_{par} is relatively small in the Gyre data set. In fact, these two "forcing variables" vary less than any of the P vs. I and biomass profile parameters

(compare the standard deviations normalized to the means in Table 2). Moreover, Fig. 6 shows that the model is quite insensitive to them. In contrast, the variability in $B_{\mathrm{T}}^{\mathrm{sat}}$, the satellite-derived *Trichodesmium* chlorophyll concentration (derived from the observed subsurface profiles and measured K_{par} values using (6)), is relatively large (Table 2). In fact it varies more than any of the P vs. I and biomass profile parameters, and Fig. 6 shows that the model is moderately sensitive to variations in this parameter. Thus, of the three forcing variables specified in the model, only variations in one, $B_{\mathrm{T}}^{\mathrm{sat}}$, has a strong influence on the estimated noon-time rates.

The insensitivity to I_0 that is apparent in Fig. 6A is due to the fact that the observed noon-time irradiances saturate the *Trichodesmium* N_2-fixation vs. I function (3) in the model throughout the upper 50 m of the water column when the average parameter values from the Gyre cruise (Table 2) are used (the cruise mean $I_k = P_{\max}^{B_{\mathrm{T}}}/\alpha^{B_{\mathrm{T}}} = 138.7 \ \mu\mathrm{E} \ \mathrm{m}^{-2} \ \mathrm{s}^{-1}$. Using the cruise mean values for I_0 and K_{par} from Table 2 in (5) gives $I(Z) = I_k$ at $Z = 49.94$ m). One would expect the
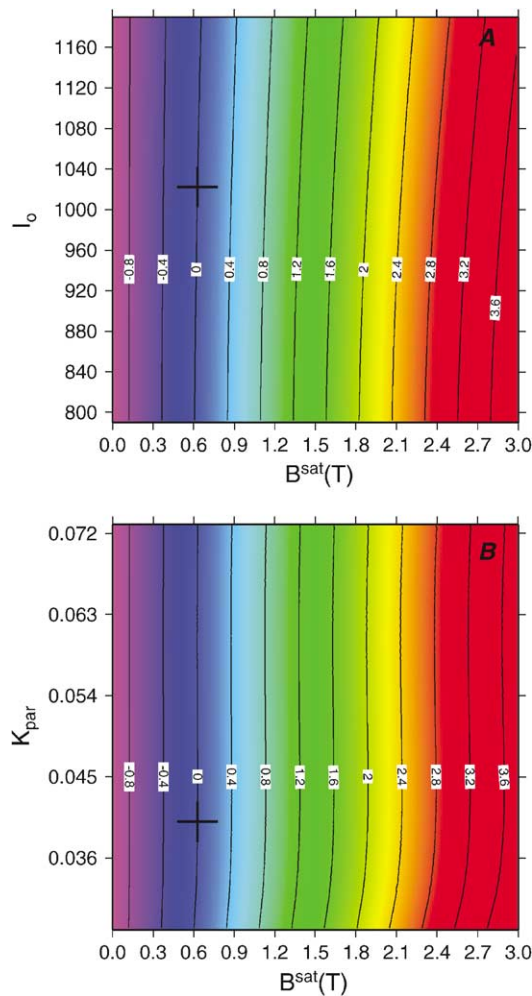

Fig. 6. As in Fig. 3 for (A) $B_{\mathrm{T}}^{\mathrm{sat}}$ vs. I_0, and (B) $B_{\mathrm{T}}^{\mathrm{sat}}$ vs. K_{par} with ranges taken from Table 2.

model to be more sensitive to variations in I_0 when integrating over the entire daylight period because the N_2-fixation vs. *I* response of *Trichodesmium* will not be as saturated in the morning and evening hours. Platt et al. (1988) show that this is, indeed, the case with their model. The immediate goal of this paper, however, is to estimate noon-time rates.

Given that the model-estimated rate is very sensitive to the depth of the subsurface biomass maximum, Z_m, it is surprising that it is so insensitive to K_{par}. Intuitively one would think that both Z_m and K_{par} determine the degree to which the subsurface irradiance profile intersects the subsurface biomass profile and that both would therefore have a strong influence on the calculated area, *h*, under biomass curve. However, inspection of (7) reveals that K_{par} is found in the same attenuation form ($e^{-2K_{par}Z}$) in the both the numerator and denominator of (7) whereas Z_m is only present in the denominator. Thus, Z_m has a strong effect upon *h* but K_{par} does not because its effect cancels. Of course, K_{par} also determines $I(Z)$ (5) and $P^{B_T}(Z)$ (3), but because the latter is saturated the effect of relatively small variations in K_{par} is not great. As with I_0, the sensitivity to K_{par} will likely increase when the model is integrated over the day.

4. Empirical estimation of $P^{B_T}_{max}$ and Z_m:

The sensitivity of the model to observed variations in $P^{B_T}_{max}$ and Z_m shows that means must be sought to account for at least some fraction of the natural variability in these two parameters. That is, if fixed values are used, in situ variability may give rise to substantial errors in the rate estimates. It also might be possible to reformulate the model so that it is less sensitive to $P^{B_T}_{max}$ and Z_m. The latter is discussed in Section 6. In this section preliminary attempts to account for natural variability $P^{B_T}_{max}$ and Z_m are described.

Previous efforts to estimate parameters in models that calculate primary production from near-surface chlorophyll concentrations have taken two basic forms. One approach is to divide the ocean into time and space domains in which the *P* vs. *I* parameters and the shape of the subsurface profile can be considered relatively constant, and then use different parameter values for different regions and seasons (e.g. Platt and Sathyendranath, 1988; Platt et al., 1991a, b; Sathyendranath et al., 1995; Longhurst et al., 1995). The other approach is to use additional data (preferably data that can be measured remotely, e.g. advanced very high-resolution radiometer (AVHRR) sea-surface temperature estimates) to help resolve the temporal and spatial variability in model parameters (e.g. Balch and Byrne, 1994; Behrenfeld and Falkowski, 1997). In this paper the latter approach is taken; i.e. a series of correlation analysis have been carried out using all of the available environmental measurements from the R.V. Gyre cruise (e.g. wind, temperature, salinity, light attenuation, location, etc.) to search for statistically significant correlations that might be exploited in the model to account for some of the variability in $P^{B_T}_{max}$ and Z_m. In this search three constraints were considered: (1) the factor under consideration must be attainable via remote sensing measurements, models or climatologies; (2) the relationship must be statistically significant; and (3) there must be at least some plausible causal link that explains why the relationship exists (the latter constraint is imposed in an effort to avoid incorporating empirical relationships into the model that have no mechanistic basis).

It should be emphasized that the relationships described in the following two subsections are exploratory; i.e. they are intended to *suggest* some possible relationships that, if they turn out to
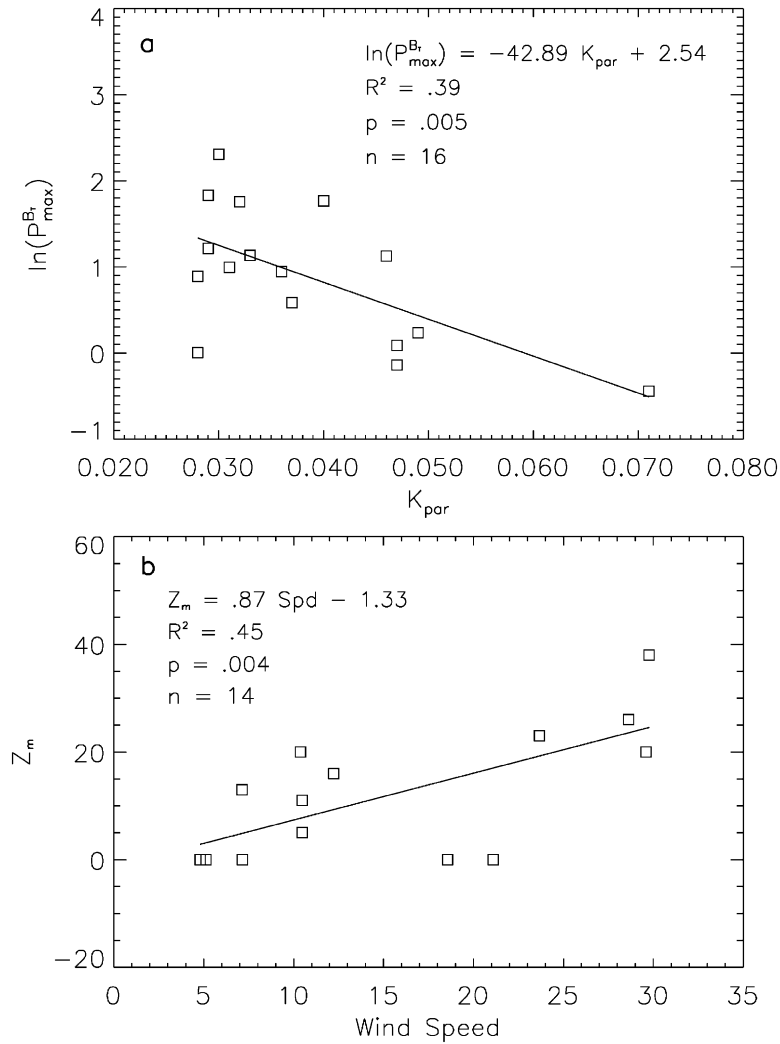
Fig. 7. Scatter plots of (A) $\ln(P_{max}^{B_T})$ vs. K_{par} and (B) Z_m vs. wind speed (in knots), with fitted (model I) regression lines. R^2 is the regression coefficient, p is the one-tailed probability that the correlation arose by chance, and n is the number of paired observations used to derive the relationship. These plots were generated using data collected on the R.V. Gyre cruise (see Section 3 for details).

be robust, might be exploited in future efforts to estimate N_2-fixation remotely. The regression equations reported in these sections and in Fig. 7 were derived using statistical analysis system (SAS) software, which uses a model I linear regression.

4.1. Estimating $P_{max}^{B_T}$ from K_{par}

In the initial search for relationships that might explain some of the variability in $P_{max}^{B_T}$, the following environmental variables were considered: surface temperature and salinity, depth of the *Trichodesmium* biomass maximum, total integrated *Trichodesmium* chlorophyll, diffuse

attenuation coefficient for PAR, average irradiance over the N_2-fixation vs. I incubation period, wind speed, and position (i.e. latitude and longitude). The results from a simple, linear correlation analysis revealed only one potentially useful relationship: a negative correlation between $P_{max}^{B_T}$ and K_{par}, with $r = -0.375$, p(one tailed) $= 0.13$. It was found that the strength of this correlation could be substantially improved by taking the natural logarithm of $P_{max}^{B_T}$, that is by assuming an exponential relationship between $P_{max}^{B_T}$ and K_{par}. This relationship

$$\ln(P_{max}^{B_T}) = -42.89 \times K_{par} + 2.54 \tag{8}$$

which is plotted in Fig. 7A, is statistically significant (p(one tailed) $= 0.005$) and explains 39% of the observed variability in $P_{max}^{B_T}$ ($r^2 = 0.39$). It is also "well behaved" because as $K_{par} \to 0.028$, $P_{max}^{B_T} \to 3.82$; and as $K_{par} \to 0$, $P_{max}^{B_T} \to 0$. Thus, the relationship will never predict unrealistically high $P_{max}^{B_T}$ values and will give 0 in turbid waters.

This relationship shows that the maximum rates of *Trichodesmium* N_2-fixation tend to be higher in clearer open-ocean waters, which is consistent with our general understanding of the ecology and physiology of this organism. That is *Trichodesmium* appears to exploit an ecological niche created by severe nitrogen limitation in oligotrophic waters, where diazotrophy confers a distinct competitive advantage over other phytoplankton species (Capone et al., 1997). However, high rates of N_2-fixation have been observed when K_{par} is relatively large (R. Letelier, pers. comm.), and it is shown below that (8) cannot be used in the SAB *Trichodesmium* bloom reported by Subramaniam et al. (2002) because the water there was more turbid than observed during the R.V. Gyre cruise. Thus, it is clear that this relationship cannot be generalized to all *Trichodesmium* blooms.

4.2. Estimating Z_m from wind speed

In an effort to find empirical relationships that explain some of the variability in Z_m, another linear correlation analysis was carried out, but in this case the environmental variables considered included only sea-surface temperature and salinity, wind speed, K_{par} and B_T^{sat}. It was found that temperature, salinity and wind speed all correlate with Z_m with probabilities between 5% and 10%, i.e., temperature vs. Z_m gives $r = -0.46$, $p = 0.08$(one tailed); salinity vs. Z_m gives $r = 0.45$, $p = 0.08$(one tailed); and wind speed vs. Z_m gives $r = 0.50$, $p = 0.06$(one tailed). Thus, deeper subsurface maxima tend to be associated with colder water, higher salinities and higher wind speeds. Only the relationship between wind speed and Z_m was explored further because it was the strongest correlation, and because the correlations with temperature and salinity can be interpreted as arising as a result of the effects of variations in surface winds (i.e. high wind speeds result in deeper mixing that both cools the surface waters and results in higher salinities).

Because the correlation between wind speed and Z_m is likely to be related to the history of the wind variability before the biomass profile was measured, a search was carried out to find the time lag (before sampling) and optimal averaging window (centered about the lag) that results in the highest correlation. This search, which was done by incrementally changing the time lag and the width of the averaging window and then plotting the resulting correlation coefficients, revealed a clear maximum in the correlation between wind speed and Z_m at a time lag of approximately 7.4 h and with an averaging window of 30 min. The resulting relationship

$$Z_m = 0.87 \times \text{SPD} - 1.33, \tag{9}$$

which is shown in the bottom panel of Fig. 7, is significant ($p = 0.004$(one tailed)), and explains 45% of the variability in Z_m ($r^2 = 0.45$). The lag of 7.4 h is likely related to the fact that the response of the mixed layer to changes in wind speed is gradual, i.e. it takes several hours of sustained winds to change the mixed layer sufficiently to impact the vertical distribution of *Trichodesmium*. Note that (9) predicts that at wind speeds at and below 1.53 knots the maximum *Trichodesmium* biomass tends to occur at the sea surface. This is consistent with numerous anecdotal field observations that suggest that surface blooms only develop when winds are light (D.G. Capone and A. Subramaniam, unpublished).

A correlation between wind speed and the depth of the *Trichodesmium* biomass maximum may be due to accumulation of colonies and/or trichomes at the base of the mixed layer, which has been observed to occur in the Pacific at the Hawaiian Ocean Time series station (Ricardo Letelier, pers. comm.; Letelier, 1994). That is, increased wind speeds lead to deeper mixed layers and therefore deeper *Trichodesmium* biomass maxima because *Trichodesmium* biomass tends to be highest at the base of the mixed layer. This relationship however, has not, been observed in the Atlantic (E. Carpenter, unpublished observations). Alternatively, the correlation between wind speed and Z_m may simply arise as a result of mixing populations over greater depths when surface winds are higher.

5. Model application in the South Atlantic Bight

In this section a test calculation is made using a remote estimate of *Trichodesmium* chlorophyll concentration in the South Atlantic Bight (off northeast Florida) from Subramaniam et al. (2002). It should be emphasized that this application does not constitute a validation of the model because no direct rate measurements were made during the SAB bloom. Rather, this calculation is intended to show how the model can be applied to calculate potential N_2-fixation rates over large spatial areas, and to determine whether or not it produces reasonable rates.

This test calculation was made using SeaWiFS data acquired at 1248 h local time on October 30, 1998. K_{par} (Fig. 8) was estimated from SeaWiFS K_{490} using an empirical relationship

$$K_{par} = 0.0304 + 0.893 \times K_{490} \tag{10}$$

derived using shipboard measurements of K_{par} and K_{490} from previous cruises in the South Atlantic Bight (J. Nelson, unpublished). *Trichodesmium* chlorophyll concentration, B_T^{sat} (Fig. 9), was estimated as described by Subramaniam et al. (2002), and $Z_m = 0.875$ m was estimated from concurrent shipboard measurements of wind speed (SPD = 2.54 knots) using (9), with a 7.4-h lag time and averaging window of 30 min, as described above. These data were then used, along with the Gyre cruise mean values of σ (from Table 2), to calculate h for each SeaWiFS pixel using (7). Then $B_T(Z)$ was estimated for each pixel according to (2).

$P^{B_T}(Z)$ was calculated with (3) using the Gyre cruise mean values for $P_{max}^{B_T}$, α^{B_T}, and I_b (from Table 2). The empirical relationship (8) between K_{par} and $P_{max}^{B_T}$ derived in section 4.1 was not used to estimate $P_{max}^{B_T}$ in this test calculation because the water in the SAB was generally more turbid than the water sampled during the R.V. Gyre cruise (see below). $I(Z)$ in (3) was calculated for each SeaWiFS pixel using (5) with K_{par} derived from SeaWiFS and I_0 ($= 1292\ \mu E\ m^{-2}\ s^{-1}$) from
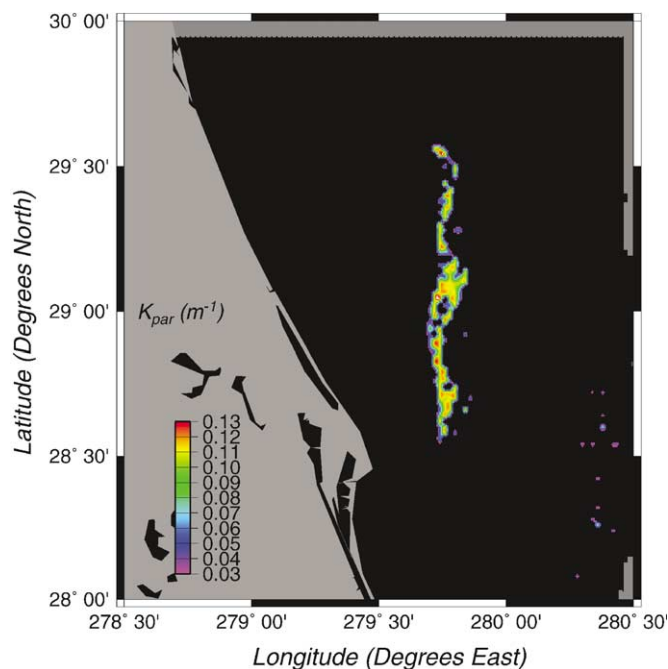
Fig. 8. Image of K_{par} in the South Atlantic Bight on October 30, 1998 estimated from SeaWiFS-derived K_{490} using Eq. (10). K_{490} was derived from the same SeaWiFS scene as described in Subramaniam et al. (2002) using the SeaWiFS Data Analysis System (SeaDAS), version 3.3 (Fu et al., 1998). The image was masked in black at *Trichodesmium* chlorophyll concentrations below 0.5 mg/m^3.

direct shipboard irradiance measurements. The latter was calculated by averaging over a 1-h time period centered at 1248 h local time, October 30th, 1998. With $B_T(Z)$ and $P^{B_T}(Z)$ specified, then the vertically integrated rate can be calculated according to (1). Each component of this calculation and the resulting rate image (Fig. 10) are discussed in more detail in the following paragraphs. All of the forcing variables and model parameters used in this test calculation are summarized in Table 3.

Fig. 9 (and Fig. 1C in Subramaniam et al., 2002) reveals a well-developed *Trichodesmium* bloom extending approximately 115 km along a front centered at about 279.75° E. longitude. As discussed in Subramaniam et al. (2002) shipboard measurements confirmed the presence of *Trichodesmium* in this area. A comparison of Figs. 8 and 9 shows that the spatial variability in K_{par} (and K_{490}) is very similar to *Trichodesmium*. Thus, *Trichodesmium* appears to have had a strong influence on the optical properties of the surface waters in the bloom. The estimated K_{par} values in the bloom region ranged from 0.03 to 0.12 m^{-1}, and 90% of them were greater than 0.071 m^{-1}, which was the highest K_{par} value measured during the R.V. Gyre cruise (Table 2). Thus, most of the K_{par} values in the SAB were greater than the highest values observed in the Gyre cruise data set (Table 2).

Fig. 10, which shows the model-estimated noon-time N$_2$-fixation rates for the SAB bloom, gives values ranging from 14 to 113 μmol N m^{-2} h^{-1}. (The low end of the calculated range of rates does
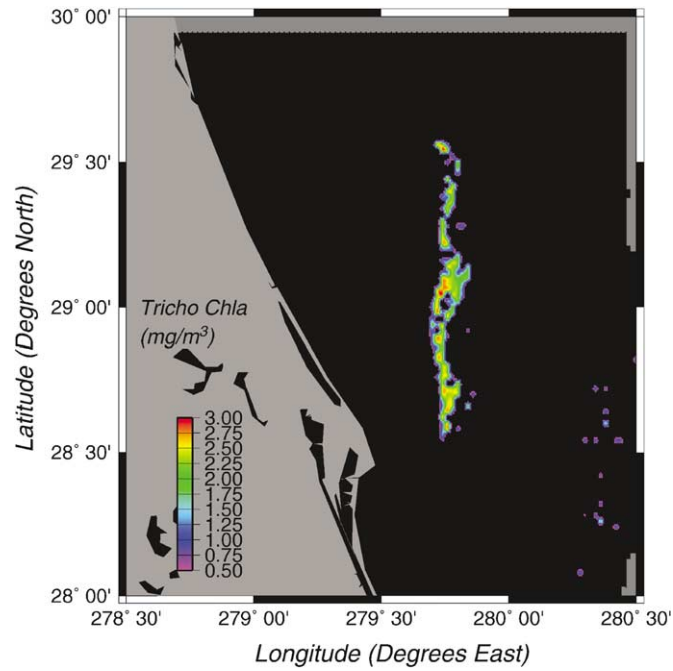
Fig. 9. As in Fig. 8 for *Trichodesmium* chlorophyll concentration estimated as described in Subramaniam et al. (2002).
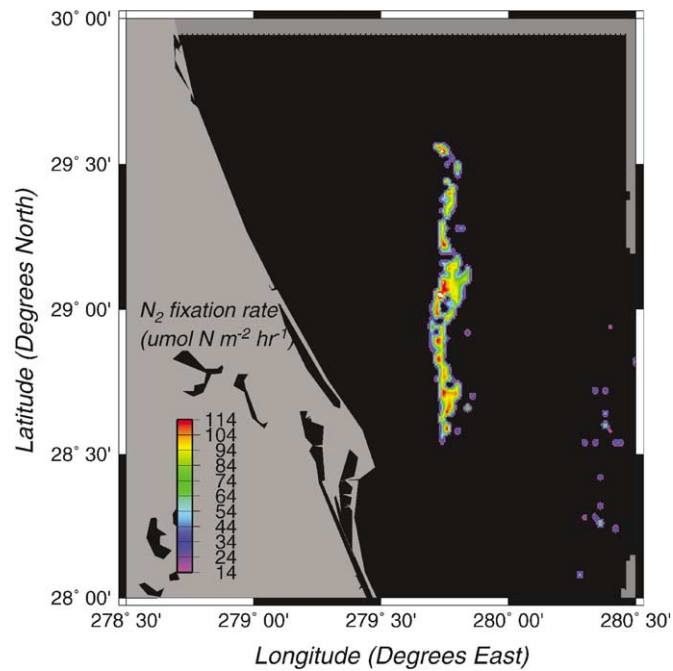

Fig. 10. As in Fig. 8 for noon-time N_2-fixation rate estimated with the model described in this paper, and using input parameters specified in Table 3.

Table 3
Forcing variables and model parameters for the South Atlantic Bight calculation

Symbol	Value and units	Source
Forcing variables		
I_0	1292.46 μE m^{-2} s^{-1}	From shipboard PAR measurements
K_{par}	0.03–0.12 m^{-1} (Fig. 8A)	Derived from SeaWiFs K_{490}[a]
B_T^{sat}	0.5–3.0 mg/m^3 (Fig. 8B)	From Subramaniam et al. (2002)
Model parameters		
$P_{max}^{B_T}$	3.19 μmol N(mg chl h)$^{-1}$	Gyre cruise mean[b]
α^{B_T}	0.023 μmol N(mg chl h)$^{-1}$(μE m^{-2} s^{-1})$^{-1}$	Gyre cruise mean[b]
I_b	1195 μE m^{-2} s^{-1}	Gyre cruise mean[b]
σ	11.132 m	Gyre cruise mean[b]
Z_m	0.875 m	From ship wind speed[c]

[a] See text, Eq. (10).
[b] See Table 2.
[c] See text, Eq. (9).

not go to zero because the SeaWiFS-estimated *Trichodesmium* chlorophyll concentrations do not go to zero; Subramaniam et al., 2002). Assuming these rates were maintained continuously over an 8-h period during the daylight hours gives a range of 112–904 μ mol N m^{-2} day^{-1}. For comparison, non-bloom measurements summarized by Capone et al. (1997) suggest rates of 0.0–8 μmol N m^{-2} day^{-1} in subtropical waters, and from 36 to 200 μmol N m^{-2} day^{-1} in tropical seas. The limited number of reports of directly determined N$_2$-fixation rates in putative blooms range from 100 to 770 μmol N m^{-2} day^{-1} (Capone et al., 2002). Considering the extreme densities reported for some blooms (Capone and Carpenter, 1982), the upper limit of the rates given here for the SAB bloom is certainly within reason, and the range is consistent with that of a modest *Trichodesmium* bloom.

As discussed above, the model rate estimates are particularly sensitive to the depth of the subsurface biomass maximum, Z_m, and the maximum rate of N$_2$-fixation, $P_{max}^{B_T}$, and N$_2$-fixation rates may be substantially overestimated if either is too large. Although the winds were variable during the time period in which the SAB bloom occurred (Subramaniam et al., 2002), they were relatively light during the early morning hours of October 30. Hence, with a 7.4-h time lag, (9) predicts a Z_m that is less than 1 m at mid-day. It is therefore unlikely that Z_m has been substantially overestimated, and if it has been underestimated the error should not be too large (Fig. 5). It is interesting to note that the direct shipboard observations from the SAB indicate that the *Trichodesmium* population densities at the sea surface responded quite rapidly to changing wind conditions (Subramaniam et al., 2002), lending further support to the potential utility of (9). Clearly, further investigations into relationships between wind speed and vertical distribution are warranted. The greatest uncertainty in the SAB bloom rate calculation is probably associated with the value of $P_{max}^{B_T}$, which could be significantly different than the mean value from the tropical Atlantic that was used in this calculation. As Fig. 3 shows, any error in the choice of $P_{max}^{B_T}$ will translate approximately into a proportional error in the estimated rate.

6. Summary and conclusions

As described by Subramaniam et al. (2002), significant progress has been made in efforts to detect and quantify *Trichodesmium* biomass using remote optical measurements. Although the semi-empirical classification scheme described there is currently specific to coastal waters, future efforts will be focusing on the development of general algorithms that can be applied globally. In this paper a simple model is described that can be used to calculate N_2-fixation rate from these remote biomass estimates, which is based upon measured *Trichodesmium* N_2-fixation rate vs. I response curves and observed subsurface biomass distributions. This effort was motivated by the need to develop alternative means for estimating global N_2-fixation rates, and the possibility that it may be feasible to estimate these rates more accurately from space than total primary production. The latter speculation stems from the fact that (1) *Trichodesmium* populations tend to reside near the surface in clear waters and can therefore be more readily remotely sensed, and (2) because the goal is to model a monospecific population that should eliminate parameter variability associated with changes in community structure. This study has shown, however, that these potential advantages do not necessarily lead to more accurate rate estimates.

The data collected on the R.V. Gyre cruise show that there is considerable variability in *Trichodesmium* N_2-fixation rate vs. I parameters in tropical Atlantic waters, i.e. more than a factor of 10 for I_b, α^{B_T} and $P_{max}^{B_T}$. This variability is comparable to that observed for production vs. I parameters in natural marine phytoplankton communities (e.g. Platt et al., 1980; their Table 2). Thus, contrary to expectation, it does not appear that consideration of a monospecific population (i.e. *Trichodesmium*) significantly reduces the variability in these parameters. Clearly, the physiological condition of these populations varies tremendously depending upon local environmental factors.

Of the three N_2-fixation vs. I parameters, the model is only sensitive to variations in $P_{max}^{B_T}$, and it is suggested that it may be possible to account for some of the variability in this parameter using empirical relationships, such as that described between $P_{max}^{B_T}$ and K_{par} in Fig. 7A (Eq. (8)). This correlation, which indicates that maximum rates of N_2-fixation tend to be higher in clearer water, is consistent with the idea that *Trichodesmium* exploits an ecological niche where a combination high light levels and extremely low inorganic nitrogen concentrations allow N_2-fixation to confer a competitive advantage over other phytoplankton species. However, this relationship could not be applied to the SAB *Trichodesmium* bloom because most of the K_{par} values there were higher than observed during the R.V. Gyre cruise. If it had been applied, 90% of the predicted $P_{max}^{B_T}$ values would have been below 0.64 μmol N(mg chl h)$^{-1}$, and the model-estimated rates would have been at least 80% lower (Fig. 3B). Thus, the relationship depicted in Fig. 7 (Eq. (8)) may not be very useful in more turbid coastal waters. Moreover, the SAB application demonstrates that the high *Trichodesmium* concentrations required for remote detection may result in K_{par} values, due to self-shading, that are generally too high to allow application of (8). Clearly, a much larger data base, spanning a wider range of optical conditions, will be required to determine whether or not such relationships can be used for predicting $P_{max}^{B_T}$.

With the exception of a few anomalous profiles that contained more than one subsurface maximum in *Trichodesmium* biomass, the vertical distribution of *Trichodesmium* is described reasonably well by a simple Gaussian function, which, when used in concert with satellite

estimates of near-surface *Trichodesmium* chlorophyll, can specify the biomass profile with only 2 parameters, σ and Z_m. The model is relatively insensitive to changes in σ over most of the observed range of variability. Thus, it is probably safe to use a fixed (i.e. mean) value for σ in the model because natural variations in this parameter should not impact the calculated rates very much except in a few extreme cases. However, the modeled rates are quite sensitive to Z_m over much of the observed range of Z_m values, and the model is particularly sensitive to cases where Z_m is overestimated. Thus, it is not advisable to use a mean value for this parameter when estimating areal rates because small deviations from this mean can severely impact the model-calculated values.

As proposed above, it may be feasible to account for at least some of the observed variability in the depth of the *Trichodesmium* biomass maximum from changes in wind speed. This approach is appealing because there is a considerable amount of evidence which suggests that *Trichodesmium* distributions are very sensitive to changes in the wind field (Capone et al., 1997; Subramaniam et al., 2002; and numerous anecdotal observations). Moreover, there are potential mechanistic explanations, such as accumulation of biomass at the density discontinuity at the base of the mixed layer due to the vertical migration behavior of *Trichodesmium*, and/or direct mixing of populations over greater depths when surface winds are higher. Because the sensitivity to Z_m is greatest in cases where the value specified in the model is deeper than the true in situ depth, it would be prudent to explore ways of insuring that the depth of the *Trichodesmium* biomass maximum is not overestimated. It is also important to consider that Z_m may vary with the time of day and perhaps even in response to ambient light levels which might have to be taken into account when calculating daily integrated rates.

In addition to the model parameters, the sensitivity analysis shows that the model is almost completely insensitive to changes in two of the forcing variables, K_{par} and I_0, over the observed range of variability. The insensitivity to I_0 is due to the fact that, with mean N_2-fixation vs. I parameters, the rates are always saturated during mid-day. The model should be more sensitive to variations in irradiance when it is integrated over the full day, and variations in I_0 will probably need to be accounted for in future applications. Although the result is counterintuitive, the lack of sensitivity to K_{par}, is explained by its presence in both the numerator and denominator of (7). It therefore, may be possible to treat this variable as a constant in the model. In contrast, the model-calculated rates are sensitive to B_T^{sat}, varying linearly in response to this forcing variable over the observed range of B_T^{sat} values (Fig. 6). Thus, there is a benefit to include remote estimates of *Trichodesmium* chlorophyll as input to the model. However, the model is equally sensitive to variations in $P_{max}^{B_T}$ and much more sensitive to variations in Z_m. For generating accurate rate estimates it may be important, at least in some circumstances, to have information about Z_m and $P_{max}^{B_T}$ than B_T^{sat}.

It should be emphasized that the model proposed here is not intended for application to *Trichodesmium* blooms where slicks have formed on the surface of the ocean, because the N_2-fixation vs. I and subsurface profile data from the 1994 Gyre cruise that were used to derive and parameterize the model do not include such cases. If it is true that these slicks represent senescent *Trichodesmium* populations, then it is likely that the chlorophyll-specific N_2-fixation rates associated with them are much lower than those depicted in Fig. 2. Fortunately, the optical signature of a *Trichodesmium* surface slick is distinct from that of a population which is distributed through the water column (Subramaniam et al., 1999b). Thus, it should be possible to

distinguish surface slicks remotely and omit them from consideration in large scale rate calculations.

It is shown in Section 5 that the model generates reasonable rates when applied to a *Trichodesmium* bloom that developed in the SAB in October, 1998. However, no direct rate measurements were made in the SAB bloom, so it is not possible to directly validate the model estimates. Our sensitivity analyses show that the modeled rates could be off by a factor of two or more, and this uncertainty does not take into account the fact that the optical conditions during the SAB bloom were generally not within the range of conditions that were encountered during the R.V. Gyre cruise. This high level of uncertainty begs the question as to whether or not the model represents a significant improvement over more simplistic rate estimates that have been carried out in the past (e.g. Carpenter and Romans, 1991). Indeed, these model-generated rates may be no more precise. However, this study clearly demonstrates the low precision of any effort to estimate rates of N_2-fixation from *Trichodesmium* biomass, and it shows the likely sources of uncertainty. That is, it is particularly important to properly represent the vertical distribution of *Trichodesmium* in the light field and account for natural physiological variability when estimating rates.

The ultimate goal of this effort is to use the approach described here to provide a new estimate of the global N_2-fixation rate. However, estimating a global rate with this model will be complicated by the fact that low *Trichodesmium* concentrations are presently undetectable using remote sensing (Subramaniam et al., 2002). Thus, it will be necessary to incorporate direct observations to account for lower, but globally significant (Capone et al., 1997), background (non-bloom) levels of N_2-fixation. As a starting point, one might calculate the total rate as a simple, linear combination of the two, i.e. the background rate estimated with the model from shipboard measurements of *Trichodesmium* concentration, and the contribution from blooms estimated from satellites. In fact, an obvious means of including background rates in the model already exists: this can be done by simply reinstating a background biomass, B_0, in (2), which varies in time and space as specified by direct shipboard measurements. As discussed in Section 3.2, reinstating B_0 also may provide the additional benefit of reducing the sensitivity of the model to changes in Z_m.

The fact remains that the model described in this paper is particularly sensitive to variations in the depth of the subsurface *Trichodesmium* biomass maximum, Z_m, and the maximum rate of N_2-fixation, $P_{max}^{B_T}$, and great care will have to be taken when specifying these in any application. Clearly, future efforts need to focus on finding ways to account for natural variability in these parameters. In addition, there may be ways to reformulate the model that reduce its sensitivity. For example, the high sensitivity to Z_m arises because a Gaussian function is used to describe the subsurface biomass distribution. There may be alternative formulations that fit the observed profiles, but reduce the sensitivity of the model to the profile parameters. There also may be feedbacks between the subsurface distribution of *Trichodesmium* and the in situ light field that are not represented in the model. For example, *Trichodesmium* populations may adjust their position (Z_m and σ) in the water column by regulating buoyancy to maintain optimal light conditions. Similarly, incorporating photoadaptive changes in the maximum rate of N_2-fixation in response to changes in the subsurface light field also might have a stabilizing effect. Incorporating these kinds of feedbacks could substantially reduce the uncertainty in the model N_2-fixation rate estimates.

Acknowledgements

References

Balch, W.M., Byrne, C.F., 1994. Factors affecting the estimation of primary production from space. Journal of Geophysical Research 99, 7555–7570.

Banse, K., Yong, M., 1990. Sources of variability in satellite-derived estimates of phytoplankton production in the Eastern Tropical Pacific. Journal of Geophysical Research 95, 7201–7215.

Behrenfeld, M.J., Falkowski, P.G., 1997. Photosynthetic rates derived from satellite-based chlorophyll concentrations. Limnology and Oceanography 42, 1–20.

Capone, D.G., Carpenter, E.J., 1982. Nitrogen fixation in the marine environment. Science 217, 1140–1142.

Capone, D.G., 1993. Determination of nitrogenase activity in aquatic samples using the acetylene reduction procedure. In: Kemp, P.F., Sherr, B.F., Sherr, E.B., Cole, J.J. (Eds.), Handbook of Methods in Aquatic Microbial Ecology. Boca Raton, Lewis Press, pp. 621–631.

Capone, D.G., Zehr, J.P., Pearl, H.W., Bergman, B., Carpenter, E.J., 1997. Trichodesmium a globally significant marine cyanobacterium. Science 276, 1221–1229.

Capone, D.G., Burns, J., Yellin, G., Carpenter, E.J., 2002. N_2 fixation and N cycling in the upper water column of the tropical N. Atlantic, in preparation.

Carpenter, E.J., Romans, K., 1991. Major role of the cyanobacterium Trichodesmium in nutrient cycling in the North Atlantic Ocean. Science 254, 1356–1358.

Carpenter, E.J., Subramaniam, A., Capone, D.G., 2002. Biomass and Primary productivity of the cyanobacterium, *Trichodesmium spp.*, in the southwestern tropical N Atlantic Ocean, in preparation.

Codispoti, L.A., 1989. Phosphorus vs. nitrogen limitation of new and export production. In: Berger, W.H., Smetacek, V.S., Wefer, G. (Eds.), Productivity of the Ocean: Present and Past. Wiley, Konferenzen, pp. 377–394.

Eppley, R.W., Petersen, B.J., 1979. Particulate organic flux and planktonic new production in the deep ocean. Nature 282, 677–680.

Falkowski, P.J., 1997. Evolution of the nitrogen cycle and its influence on biological sequestration of CO_2 in the oceans. Nature 387, 272–273.

Fu, G., Baith, K.S., McClain, C.R., 1998. SeaDAS: The SeaWiFS Data Analysis System. Proceedings of the Fourth Pacific Ocean Remote Sensing Conference, Qingdoa, China, July 28–31, 1998, pp. 73–79.

Galloway, J.N., Schlesinger, W.H., Levy II, H., Michaels, A., Schnoor, J.L., 1995. Nitrogen fixation: anthropogenic enhancement-environmental response. Global Biogeochemical Cycles 9, 235–252.

Goffman, C., 1962. Preliminaries to functional analysis. In: Buck, R.C. (Ed.), Studies in Modern Analysis, Vol. 1. The Mathematical Association of America, Prentice-Hall, Englewood Cliffs, NJ, 182 pp.

Gordon, H.R., Clark, D.K., 1980. Remote sensing optical properties of a stratified ocean: an improved interpretation. Applied Optics 19, 3428–3430.

Gruber, N., Sarmiento, J.L., 1997. Global patterns in marine nitrogen fixation and denitrification. Global Biogeochemical Cycles 11, 235–266.

Hood, R.R., Michaels, A.F., Capone, D.G., 2000. Answers sought to the enigma of marine nitrogen fixation. EOS 81, 133, 138–139.

Karl, D., Letelier, R., Tupas, L., Dore, J., Christian, J., Hebel, D., 1997. The role of nitrogen fixation in biogeochemical cycling in the subtropical North Pacific Ocean. Nature 388, 533–538.

Letelier, R., 1994. Studies on the ecology of *Trichodesmium spp.* (Cyanophyceae) in the Central North Pacific Gyre, Ph.D. Thesis, University of Hawaii.

Longhurst, A., Sathyendranath, S., Platt, T., Caverhill, C., 1995. An estimate of global primary production in the ocean from satellite radiometer data. Journal of Plankton Research 17, 1245–1271.

Michaels, A.F., Olson, D., Sarmiento, J.L., Ammerman, J.W., Fanning, K., Jahnke, R., Knap, A.H., Lipschultz, F., Prospero, J.M., 1996. Inputs, losses and transformations of nitrogen and phosphorus in the pelagic North Atlantic Ocean. Biogeochemistry 35, 181–226.

Platt, T., Gallegos, C.L., Harrison, W.G., 1980. Photoinhibition of photosynthesis in natural assemblages of marine phytoplankton. Journal of Marine Research 38, 687–701.

Platt, T., Sathyendranath, S., Caverhill, C.M., Lewis, M.R., 1988. Ocean primary production and available light: further algorithms for remote sensing. Deep-Sea Research 35, 855–879.

Platt, T., Sathyendranath, S., 1988. Oceanic primary production: estimation by remote sensing at local and regional scales. Science 241, 1613–1620.

Platt, T., Sathyendranath, S., Ravindran, P., 1990. Primary production by phytoplankton: analytic solutions for daily rates per unit surface area of water surface. Proceedings of the Royal Society of London 241, 101–111.

Platt, T., Bird, D.F., Sathyendranath, S., 1991a. Critical depth and marine primary production. Proceedings of the Royal Society of London 246, 205–217.

Platt, T., Caverhill, C., Sathyendranath, S., 1991b. Basin-scale estimates of oceanic primary production by remote sensing: the North Atlantic. Journal of Geophysical Research 96, 15 147–15 159.

Sathyendranath, S., Platt, T., 1988. The spectral irradiance field at the surface and in the interior of the ocean: a model for applications in oceanography and remote sensing. Journal of Geophysical Research 93, 9270–9280.

Sathyendranath, S., Platt, T., Caverhill, C.M., Warnock, R.E., Lewis, M.R., 1989. Remote sensing of oceanic primary production: computations using a spectral model. Deep-Sea Research 36, 431–435.

Sathyendranath, S., Longhurst, A., Caverhill, C.M., Platt, T., 1995. Regionally and seasonally differentiated primary production in the North Atlantic. Deep-Sea Research 42, 1773–1802.

Subramaniam, A., Carpenter, E.J., Karentz, D., Falkowski, P.J., 1999a. Bio-optical properties of the marine diazotrophic cyanobacteria Trichodesmium spp. I. Absorption and photosynthetic action spectra. Limnology and Oceanography 44, 608–617.

Subramaniam, A., Carpenter, E.J., Falkowski, P.J., 1999b. Bio-optical properties of the marine diazotrophic cyanobacteria Trichodesmium spp. II. A reflectance model for remote sensing. Limnology and Oceanography 44, 618–627.

Subramaniam, A., Brown, C.W., Hood, R.R., Carpenter, E.J., Capone, D.G., 2002. Detecting Trichodesmium blooms in SeaWiFS imagery. Deep-Sea Research II 49, 107–121.

Tyrrell, T., 1999. The relative influences of nitrogen and phosphorus on oceanic primary production. Nature 400, 525–531.